EEET ECOLOGICAL ENGINEERING & ENVIRONMENTAL TECHNOLOGY

Ecological Engineering & Environmental Technology 2024, 25(9), 163–173
https://doi.org/10.12912/27197050/190631
ISSN 2299–8993, License CC-BY 4.0

Received: 2024.06.10
Accepted: 2024.07.10
Published: 2024.08.01

Detection of Potentially Ore-Bearing Hydrothermal Alteration Zones in the Rehamna Massif (Morocco)

Mohamed El-Mimouni[1*], Abdellatif Aarab[1], Abdellah Lakhloufi[1], Abderrazak Hamzaoui[2], Ayoub Aabi[1], Kawtar Benyas[1]

[1] Laboratory of Analysis and Modelling of Water and Natural Resources, Mohamed V University in Rabat, Morocco
[2] National Office of Hydrocarbons and Mines (ONHYM), Rabat, Morocco
* Corresponding author's e-mail: elmimouni2@gmail.com

ABSTRACT

This study aims to map minerals of hydrothermal alteration zones in the Rehamna Massif, formerly site of large exploitation of Pb-Zn, Ba-Pb and W-Sn hosted within the Paleozoic basement, using the advantages of remote sensing technique. In this regard, ASTER remote sensing data have been used as a substrate for spectral processing, namely band ratios, to identify hydrothermal alteration zones characteristic of polymetallic mineralization. Band ratio technique leads us to map the Phyllic, Argillic, Prophylitic, Oxidation and kaolinite zones. Other ratios such as Muscovite, Allunite, Calcite and Fe-oxides were also computed. The areas reported were locally compared with the geological setting. The compilations of the results facilitate the identification of eight potential sites suitable for a possible tactical research phase. These results can encourage mining exploration and guide mining companies to the most potentially ore-bearing sites and support the economic development of the Rehamna area.

Keywords: Rehamna massif, remote sensing, ASTER data, band ratios, hydrothermal alteration, potential sites.

INTRODUCTION

To support their economic rise, many countries recur to the mining sector and advance exploration programs for their mineral resources. In Morocco, most mining activity is concentrated in the Anti-Atlas metallogenic belt and Western Meseta domain and well-studied from a geological and metallogenic context (Tuduri et al., 2018; Aabi et al., 2021; Samaoui et al., 2023). In this last zone, almost mineral deposits are belonging to three famous Hercynian Massifs: Morrocan Central Massif, Jebilet Massif and Rehamna Massif.

Except the Rehamna inlier, several mining sites are stilling in operation in Morrocan Central Massif: El Hammam, Achemmach mines (Ba, Sn), polymetalic site of Tighza (Pb, Ag, Cu, Zn, Au), and several volcanologic massif sulfied mines belonging to Jebilet inlier mininig Zn, Pb and Cu (Bouabdellah and Slack, 2016; Mahjoubi, 2017). In the the Rehamna inlier, outcrops of granitoids were accompanied by hydrothermal alteration, especially around the leucogranite apexes, and lead mining Sn, W, Pb, Cu, and Mo. Silicification, greisenisation, oxidation and chloritisation around the leucogranitic apexes, and in the location of presumed ones, indicate the expression of this phenomenon (El Mahi et al., 2000 and references therein, El Mimouni et al., 2022). In similar contexts, mapping of alteration zones is among the first steps in mining research programs (Rowan et al., 2005; El Janati, 2019).

The effectiveness of remote sensing images and techniques in several fields essentially in geological studies such as lithological mapping, mineral discrimination and hydrothermal alteration minerals delineating give excellent results at different scales (Ramadan and Kontny, 2004; Akbari et al., 2015; Zhang et al., 2016).

Remote sensing images and applications have a paramount role for geological investigations of developing states and for probable financiers in mineral investigation sector (Rokos et al. 2000). Identification of hydrothermally altered host rocks is a key to the strategic phase of mining research (Rani et al., 2020). Currently, multispectral and hyperspectral sensors by their wide spectral range can target minerals of hydrothermal alterations, namely Allunite, Kaolinite, chlorite, and Epidote (Gabr et al., 2010; Lamrani et al., 2021). It represents a practical tool that can help to make decisions.

In the Rehamna Massif, the mining field was one of the fundamental pillars of the regional economy. Therefore, the main aim of this work consists of research for new promising sites through mapping of hydrothermal alteration minerals related to ore-bearing rich zones. To achieve this objective, we propose a synergy of Advanced Spectral Thermal Emission and Reflection Radiometer (ASTER) data analyses and fieldwork data. Reminding us that in the Rehamna inlier, we are in a Hercynian geodynamic context which is linked in other similar areas to significant mining potential

REGIONAL GEOLOGICAL SETTING

Western Meseta of Morocco

Flanked by Anti Atlas and Rif belts, the Meseta domain corresponds to the Paleozoic basement unconformably surrounded by Mesozoic-Cenozoic covers, deformed intensively by the Hercynian (Variscan) orogeny (Lakhloufi, 2002, Hoepffner et al., 2017) and partially by the Alpine orogenic cycle (Bouazzama et al., 2023). The middle Atlas belt spears the eastern Meseta and the western one (Fig. 1). Three famous massifs belonging to the western Meseta, from northern to southern we distinguish; Moroccan Central Massif, Rehamna and Jebilet Massifs (Fig. 1). In the south of the Jebilet Massif, we come across the High Atlas Paleozoic block.

Rehamna Massif

The Rehamna Massif is one of the principal Palaeozoic blocks of Moroccan Hercynian belt,

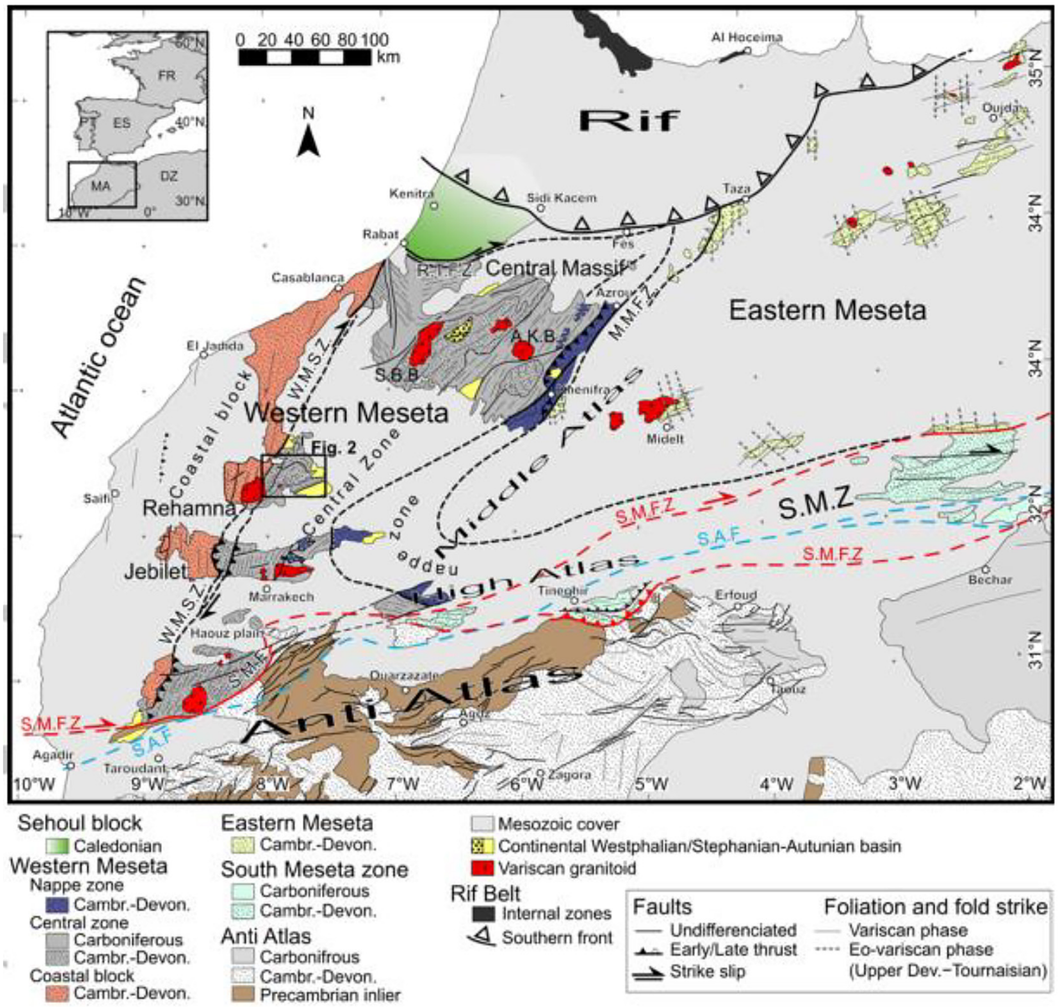

Figure 1. Structural map of the Moroccan Variscides (Chopin et al. 2014, modified after Michard et al., 2010)

composed of two parts geologically and structurally distinguished; the Northern part labeled also Machraa Ben Abbou Basin (MBAB), and the southern part or Rehamna Massif. The MBAB consists of Lower Devonian to upper Visean terrains that contain numerous magmatic rocks, mostly gabbros, dolerite, and basalts (Kholaiq, 2017). However, the Rehamna inlier s.str is consist of Precambrian to Permian formations, intruded by different magmatic acidic outcrops; it contains the oldest rocks known in the mesetean domain represented by rhyolitic outcrops of paleoproterozoic age (Pereira et al., 2015). Three most important structural parts have been identified in the Rehamna Massif (Fig. 2), separated by the median fault and the major fault of Oulad Zednes, parts of the Western Meseta Shear Zone (El Mahi et al., 2000; Michard et al., 2010).

- The western Rehamna, which belongs to the Coastal Bloc, is considered as the least deformed zone of the Moroccan Meseta. This region is limited by the NE median fault to the East were outcrops the Sebt Lbrikiine batholith, and consists of Cambro-Ordovician terrains. The deformation increases towards its eastern edge (Michard et al., 2010).
- Central Rehamna: in this NE-SW band, the Paleozoic package overlain the Neoproterozoic basement of Central Rehamna, with an angular unconformity (El Attari 2001, Hoepffner et al., 2006). The lower Cambrian began with a detrital series (i.e., arkoses and conglomerates), covered by middle Cambrian limestones and cipolin, in turn, overlain by Devonian meta-conglomerate of kef Elmounib and Skhour formation (i.e., phyllites and quartzites) (Piqué et al., 1982; Michard et al., 2010).
- Eastern Rehamna, the region bounded to the west by the Oulad Zednes fault, and represented by metamorphic units; from north to south, we distinguish upper units of Drioukat, Allahia, and Jbel Kharrou formations dated back to Ordovician - Carboniferous, and lower units of Lalla Tittaf and Ouled Hassine.

LOCAL GEOLOGICAL SETTING

In the Rehamna Massif, the mineralization has a Hercynian to late Hercynian age of hydrothermal and pneumatolytic origin (Jenny, 1974; El Mahi et al., 2000). Ore deposits are often produced by fluid flow processes of leucogranitic apexes giving rise to vein-type deposits based on Mo, Pb-Zn, Cu, Sn, and Be. Three famous

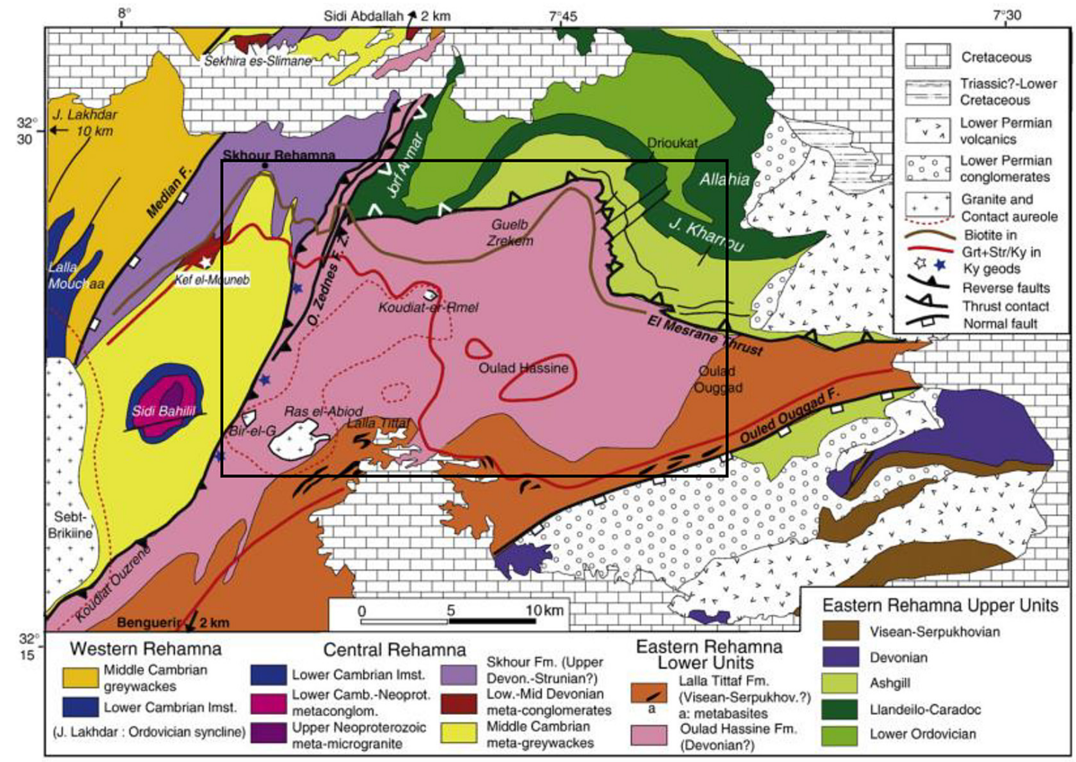

Figure 2. Simplified geologic map of Rehamna Massif (Michard, 2010, modified after Baudin et al. 2003 and Razin et al., 2003), black rectangle shows the location of the study area

peraluminous leucogranites are known in the Eastern Rehamna (Fig. 3) named: Ras Al Abiod, Bled El Gourda, and Koudiat Rmel.

Furthermore, we distinguish the leucogranite of Sidi Bahilil 1.5 km at SW of Begarat Chaâbe area, the leucogranite of Braîla, 7 km at SE of Hassine mine and aplopegmatite veins of Oulad Hassoune.

It is probable that the small leucogranite apexes of Bled El Gourda, Sidi Bahilil, and Koudiat Rmel and the alopegmatite veins constitute with the Ras el Abiod massif the outcropping part of a vast leucogranitic batholith mostly hidden at depth, as evidenced by the aureole thermal metamorphism (Baudin et al., 2003).

Hydrothermal and pneumatolytic phenomena generated by these magmatic rocks are expressed according to five aspects:

- Silcification: Silica veins are extremely abundant in the study area, indicating a significant degree of hydrothermal fluid circulation (Figure 4a). These veins, which cut both the Precambrian and Paleozoic basements, exhibit several directions with a WNW-ESE dominant one.
- Greisenization: It corresponds to a process of hydrothermal alteration in which muscovite and feldspar are transformed into hydroxylated minerals (greisens). Many greisens veins are known in the leucogranites of eastern Rehamna.
- Oxidation: the degree of oxidation is striking in the Rehamna inlier (Figures 4a and 4b); it is marked by the presence of ferrous veins (hematite and goethite).
- Tourmalinization: is a known pneumatolytic process strongly linked with Sn-W mineralization related to granite intrusions (Taylor, 1979; Pirajno, 2009). It's characterized by the replacement of feldspar and mica by tourmaline mineral, and expressed in the area of study by the presence of tourmaline associated to silica veins.
- Muscovitisation: A type of hydrothermal alteration characterized by the accumulation of muscovite, associated with biotite, feldspar, and plagioclase (Cobbing et al., 1992).

DATA AND METHOD

To carry out our subject, the use of synoptic data covering our area of study is essential. In this regards, we chose a multispectral image of Advanced Spectral Thermal Emission and Reflection Radiometer

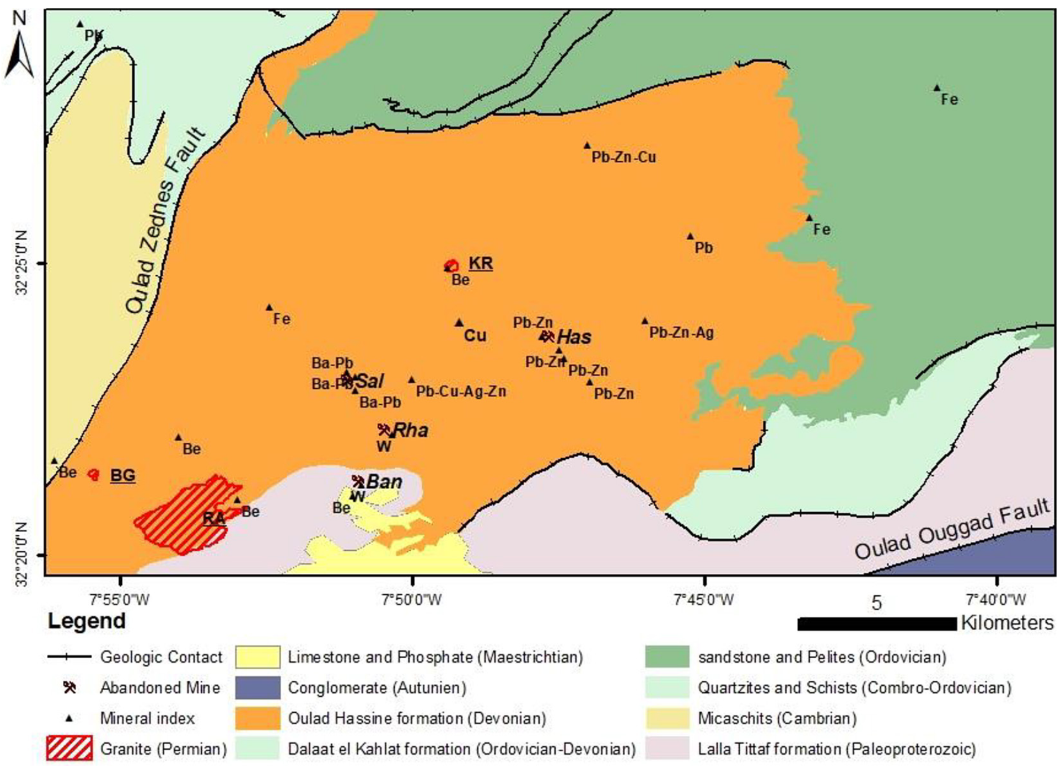

Figure 3. Simplified geological map of studied area, shows leucogranites emplacement and mineral occurrences (RA: Ras elAbiod, BG Bled El Gourda, KR: Koudiat Rmel) and abandoned mines (Has: Hassine, Sal: Oulad Saleh, Rha: Rhaichet, Ban: el Bandira) (modified after Baudin et al., 2003, Razin et al., 2003)

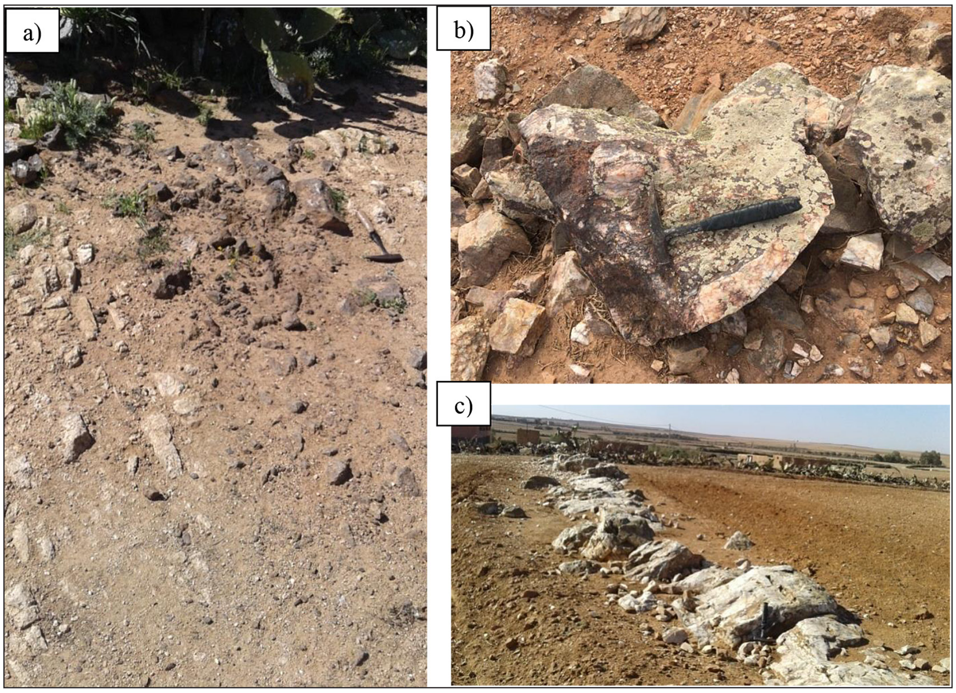

Figure 4. Field investigation Photographs: (a) N100-oriented Hematite veins, (b) oxidation in silica vein, (c) N100-oriented silica vein

(ASTER), recognized for its wide spectral range and its capacity to identify altered minerals.

ASTER data used is Level-1T, acquired on 29 April 2002, and previously corrected geometrically, calibrated radiometrically, and scaled radiance at the sensor on 2015. It includes fourteen spectral bands with three visible near-infrared (VNIR) bands (wavelength range: 0.52–0.86 µm, spatial resolution: 15 m), six short wave infrared (SWIR) bands (wavelength range: 1.6–2.43 µm, spatial resolution: 30 m), and five TIR bands (wavelength range: 8.12–11.65 µm, spatial resolution: 90 m). The ASTER data was also projected to the UTM projection (WGS84 datum, zone 29N). VNIR and SWIR bands were resampled to 15m resolution using the nearest neighbor method. Table 1 gives details of ASTER data processed in this study. A subset from the whole scene extends between latitudes 32°19’38,54”N and 32°29’19,41”N, and longitudes 7°38’59,82”W and 7°56’16,90”W covering only the study area was extracted (Figure 5), corresponding to eastern part of Central Rehamna and almost part of Western Rehamna, with an area of about 486 sq km (27 km length × 18 km width). Area of study is characterized by arid climate and a poor vegetation cover which facilitates its remote sensed study. Furthermore, the image selected does not include cloud cover.

Table 1. Spectral passbands of ASTER image

Data product		” AST_L1T_00304292002112252_20150422043455_42792”	
Subsystem	Band no.	Spectral range (µm)	Spatial resolution (m)
VNIR	1 2 3N	0.52–0.60 0.63–0.69 0.76–0.86	15
SWIR	4 5 6 7 8 9	1.60–1.70 2.145–2.185 2.185–2.225 2.235–2.285 2.295–2.365 2.360–2.430	30
TIR	10 11 12 13 14	8.125–8.475 8.475–8.825 8.925–9.275 10.25–10.95 10.95–11.65	90

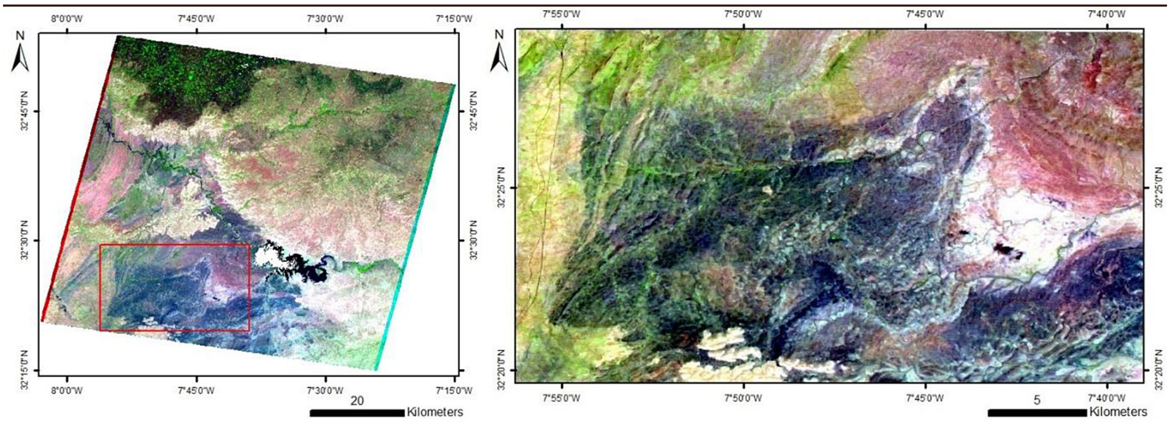

a) b)

Figure 5. a) ASTER image (RGB 4-3-2), red rectangle area of interest detailed on b)

The methodology adopted in our investigation consists of applying the band ratios to VNIR and SWIR bands of the ASTER data (Table 2). The obtained maps were superimposed on the available geological maps to get the potential mining sites with high spectral mining related to hydrothermal alterations.

DATA PROCESSING

In our case study, we used the band ratios performed by Rowan et al. (2003) as following formula: (Band 5+Band 7)/(Band 6), (Band 4+Band 6)/(Band 5), (Band 7+ Band 9)/(Band 8), and (Band 5)/(Band 3)+(Band 1)/(Band 2) to delineate respectively the phyllic zone (Sericite, Muscovite, Illite, Smectite), the argillic zone (Allunite, Kaolinite, Pyrophylite), the prophylactic zone (Carbonate, Chlorite, Epidote) and the oxidation zone (Fe^{2+}). We also applied the indices of Kaolinite and Muscovite (Band 4)/(Band 6), and Fe – oxides (Band 3)/(Band 1) approved by Testa et al. [2018].

On the other hand, we tested the following band ratios proposed for arid-semiarid regions by Ninomiya et al. [2003]:

Table 2. Examples of Band Ratio and hydrothermal alteration discrimination

Alteration minerals	Band ratio	Reference
Argillic zone	(Band 4 + Band 6) / Band 5	Rowan et al., 2003
Prophylactic zone	Band 7 + Band 9) / Band 8	
Oxidation zone	(Band 5 / Band 3) + (Band 1 / Band 2)	
Phyllic zone	(Band 5 + Band 7) / Band 6	
Mineral alteration index (OHI)	$(Band7\ /Band6) *$ (Band4/ Band6)	Ninomiya et al., 2003
Kaolinite index (KLI)	$(Band4/\ Band5) *$ (Band8/ Band6)	
Calcite index (CLI)	$(Band6\ /Band8) *$ (Band9/ Band8)	
Allunite index (ALI)	$(Band7/Band5) *$ (Band7/Band8)	
Gossan/ Iron oxides	band 4/2	Kaliknowski and Oliver, 2004 Abdelkareem et al., 2017
Aluminum hydroxide (Al-O-H)	band 4/6	Abuzied et al., 2016; Abdelkareem et al. 2017
kaolinite/Muscovite as OH-bearing	band 4/6	Testa et al. 2018
Fe-oxides	band 3/1	
Aalteration minerals with Al-OH and Fe-OH	band 4/7	Abuzied et al., 2016
Ferric oxides	band 4/3	Abdelkareem et al., 2017
Chlorite	band 5/8	Elsaid et al., 2014
Muscovite	band 5/6	Kaliknowski and Oliver 2004
Silica, Si-rich minerals	13/10	Kaliknowski and Oliver, 2004; Cudahy, 2011

$$(\text{Band }7)/(\text{Band }6)\times(\text{Band }4)/(\text{Band }6)=\text{OHI} \quad (1)$$

$$(\text{Band }4)/(\text{Band }5)\times(\text{Band }8)/(\text{Band }6)=\text{KLI} \quad (2)$$

$$(\text{Band }6)/(\text{Band }8)\times(\text{Band }9)/(\text{Band }8)=\text{CLI} \quad (3)$$

$$(\text{Band }7)/(\text{Band }5)\times(\text{Band }7)/(\text{Band }8)=\text{ALI} \quad (4)$$

where: *OHI* is the mineral alteration index, *KLI* is the Kaolinite index, *CLI* is the index of Calcite, and *ALI* is the Allunite index. Figure 6 displays the results of these processes.

RESULTS AND DISCUSSIONS

The different band ratios tested on the VNIR and SWIR bands give different spatial distributions on the zones likely to contain minerals of hydrothermal alterations. Figure 5 reveals the results of this processing dropped on band 1 of the studied ASTER image, showing also the emplacement of old mining sites, and leucogranitic apexe locations.

The phyllic zone and Kaolinite – Muscovite index show distribution in the northern part of the study area relate to Ordovician upper units of eastern Rehamna and in the Devonian formation of Skhour of Central Rehamna. The argilic zone shows the same distribution of the last index with an extension to lecogranitic outcrops. The Prophylitic zone is dependent essentially on Oulad Hassin unite where outcropping the leucogranitic apexes. The oxidation zone distribution is focused on the Jebel Kharrou

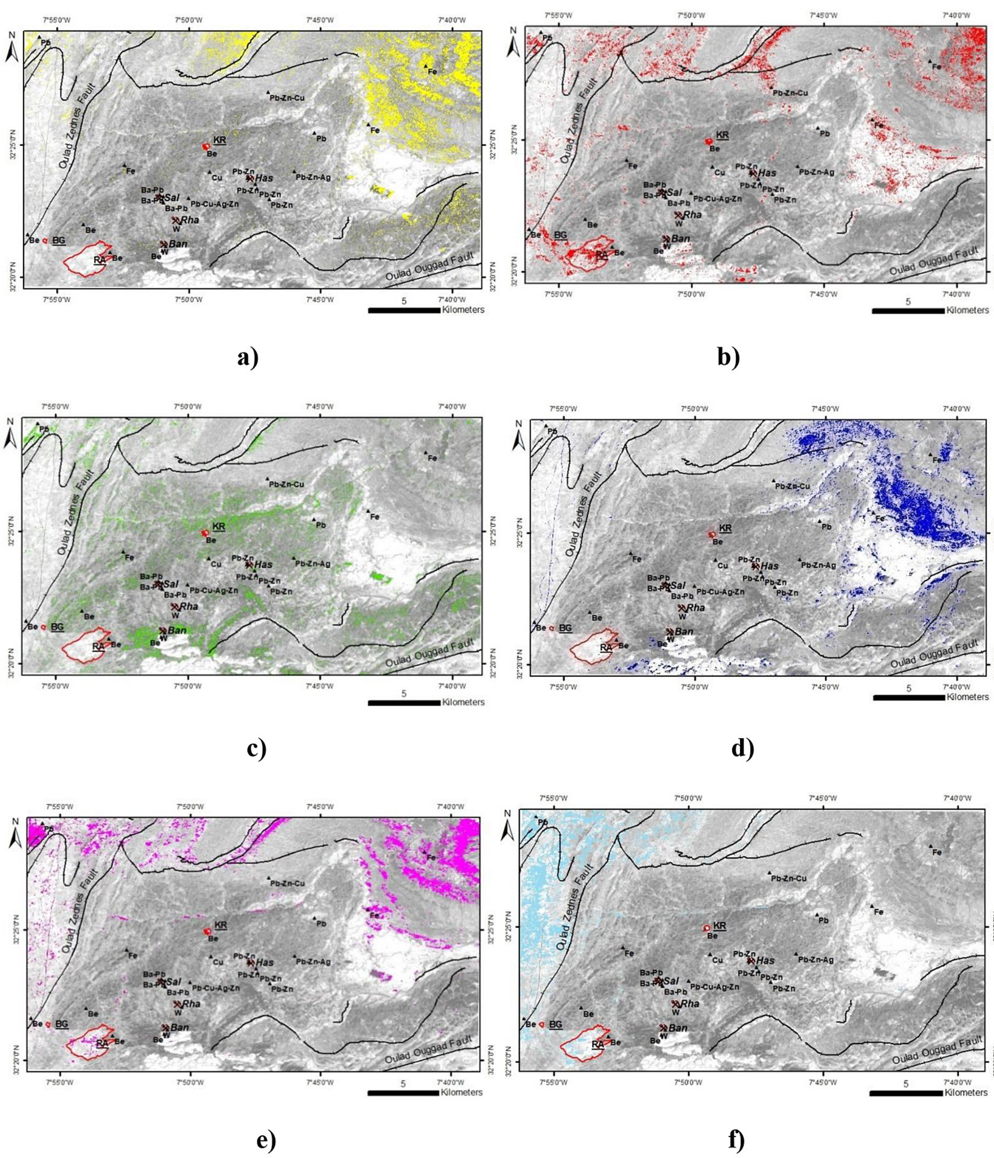

Figure 6. Results of band ratios processing: a) Phyllic zone, b) Argillic zone, c) Prophylitic zone, d) Oxidation zone e) Kaolinite – Muscovite f) (Band3)/(Band1): Fe-oxides. Granites of: RA: Ras el Abiod, SBH: Sidi Bahilil, KR: Koudiat Rmel. Mines of: Has: Hassine, Sal: Oulad Saleh, Rha: Rhaichet, Ban: el Bandira.

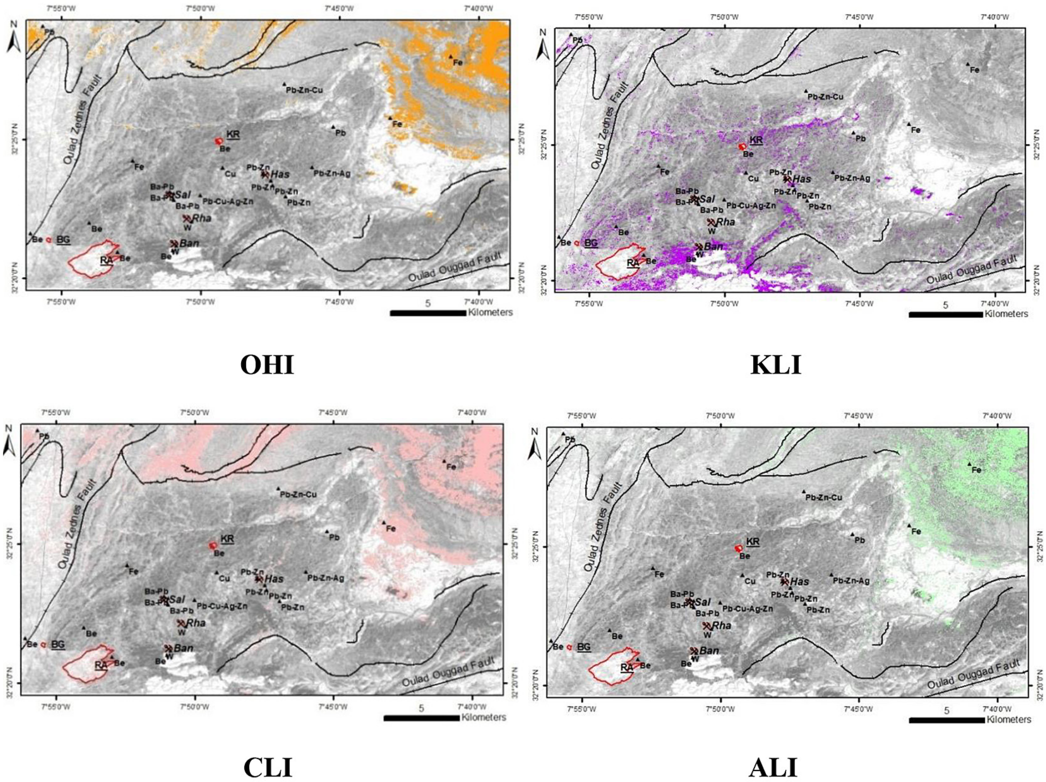

Figure 7. Results of Ninomya's band ratios processing; OHI: (Band7/Band6)*(Band4/Band6), CLI: (Band6/Band8)*(Band9/Band8), KLI: (Band 4/ Band 5)*(Band8/Band 6), ALI: (Band 7/ Band 5)*(Band 7/ Band 8)

formation, whereas the Fe oxides ratio refers to Central Rehamna. Regarding the results of Ninomya's index (Figure 6), we notice that the mineral alteration ratio (OHI) reveals the same distribution of Phyllic zone index, the Calcite index (CLI) gives a similar dispersal of Prophylitic zone, the kaolinite index (KLI) show a comparable distribution of Kaolinite-Muscovite index, were the Allunite index (ALI), display dissemination in the north-eastern part of studied area concerning Ordovician units. To achieve our purpose of the study, we brought together all the results of previous alterations with local geological settings on a Geographic Information System (GIS) to combine all layers of results and sort areas of hydrothermal alterations (Figure 7). The selected areas of potential mining interest are those that bring together the most hydrothermal alterations. The high-potential zones in the chosen sites are those that include hydrothermal alterations, mineral occurrences, and magmatic components (Figure 8).

- Site (a): in SW of Skhour Rehamna village (SR): this area includes all alterations studied according to a rounded shape, with a poor representation of Allunite, Calcite, and Oxidation indices. We notice also the occurrence of the Pb index in the border of this shape.
- Site (b): shows several alterations around Jorf el Beida (JB), essentially Kaolinite index (KLI), Argillic zone, Fe oxides, and Al-OH. The alterations distribution is according to a NE-SW direction.
- Site (c): koudiat Rmel granite is distinguished by four ratios; KLI, Argillic zone, AL-OH, and OHI. In this magmatic outcrop, we notice the presence of Be index; Contact metamorphism, and hydrothermal alterations such as tourmalinization, muscovitisation and greisenisation.
- Site (d): Oulad Hassine area contains four alterations; CLI, prophylactic zone, Fe-Oxides, and Argillic zone. This site includes also the abandoned Hassine mine (Has) where the Pb-Zn Mineralization vein type was exploited.
- Sites (e) and (f): the site (e) is located in the south of Guelb Boualla (GB), and the site (f) is in the SW of Menaat (MN). These two sitesshowalmost all studied hydrothermal alterations except the Fe-Oxides. In addition to these alterations, the El Menaat site includes a Fe index.
- Sites (g) and (h): the site (g) is situated in the West of Allahia massif (AL), and the site (h) is

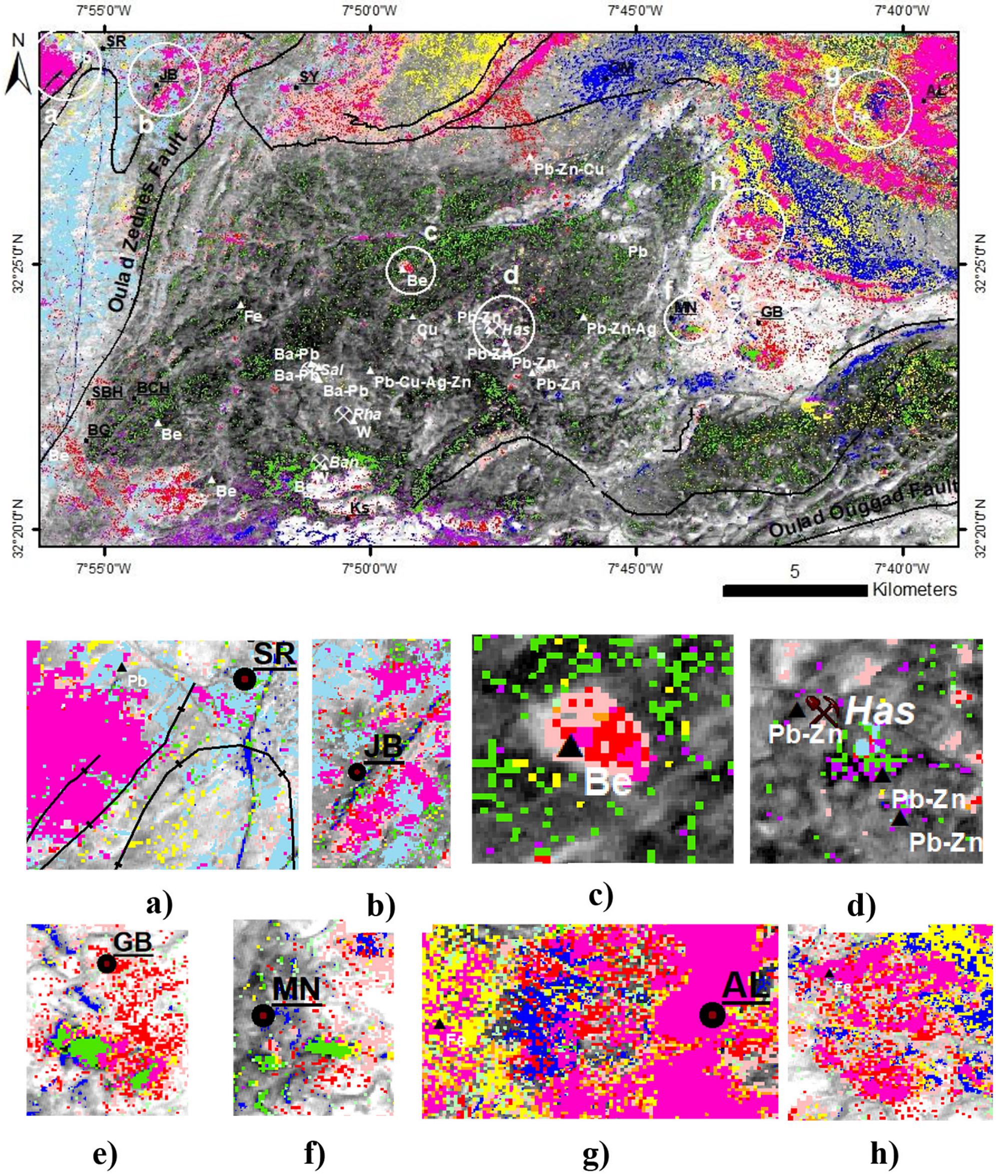

Figure 8. Results of hydrothermal alterations mapped superimposing on the band 1 of ASTER image White circles represent selected areas of potential mining interest, (a) to (h) zoomed images of areas selected.

in the NE of Rehamna Massif. These two locations display almost all ratios processed, except Fe-Oxides, Prophylactic zone, and CLI. In this last zone, we notice thepresence of Fe index and hematite ferrous minerals which are best developed in the Al-Hayar – El-Ouenkel Massifs (Hoepffner, 1974)

CONCLUSIONS

Our study was based on hydrothermal alterations mapping in the eastern part of Rehamna massif s.str belonging to the western Meseta of Morocco, using ASTER data and field investigations. Band ratio discrimination applied to SWIR and VNIR bands leads us to delineate the distribution of several hydrothermal alterations in the studied area.

The compilation of the results with field setting allows us to select eight potential mineralized areas. Almost hydrothermally altered sites selected are in concordance with mineral occurrences distribution and emplacement of known and presumed leucogranites apexes. Areas delineated need focused prospection to highlight its mining potential. The findings of the present investigation, based on hydrothermal alterations mapping, can constitute a roadmap for prospection programs and sustain the economic rise in the Rehamna district through mining exploration projects. Our approach is also favourable for being duplicated in other areas. In fact this could create an exploitable data bank in the big data sense in similar Hercynian zones.-

Acknowledgement

The authors are very grateful to the anonymous Reviewers, the Managing Editor, and the Technical Editors for their great efforts and precious comments.

REFERENCES

1. Aabi, A., Baidder, L., Hejja, Y., El Azmi, M., Nait Bba, A., Otmane, Kh. 2021. The Cu-Pb- Zn-bearing veins of the Bou Skour deposit (Eastern Anti-Atlas, Morocco): structural control and tectonic evolution. Comp. Rendus Geosci. Sci. Planet, 353, 81–99. https://doi.org/10.5802/crgeos.54
2. Abdelkareem, M., Othman, I., KamalElDin, G. 2017. Lithologic mapping using remote sensing data in Abu Marawat Area, Eastern Desert of Egypt. International Journal of Advanced Remote Sensing and GIS, 6, 2171–2177.
3. Abuzied, S.M., Ibrahim, S.K., Kaiser, M.F., Seleem, T.A. 2016. Application of remote sensing and spatial data integrations for mapping porphyry copper zones in Nuweiba Area. Egypt Int J Signal Process Syst 4(2), 102–108. https://doi.org/10.12720/ijsps.4.2.102-108
4. Akbari, Z., Rasa, I., Mohajjel, M., Adabi, M.H., Yarmohammadi, A. 2015. Hydrothermal alteration identifcation of Ahangaran deposit, West of Iran using ASTER spectral analysis. Int Geoinform Res Dev J 6(1), 28–42.
5. Baudin, T., Chévremont, P., Razin, P., Youbi, N., Andries, Hoepffner, C., Thiéblemont, D., Chihani, E.M., Tegyey, M. 2003. Carte Géologique du Maroc au 1/50 000 : Feuille de Skhour des Rehamna – Mémoire explicatif. Notes Mém. Serv. Géol. Maroc, 435, 114.
6. Bouabdellah, M., Slack, J.F. 2016. Geologic and metallogenic framework of North Africa. Mineral Deposits of North Africa. Mineral Resource Reviews, Springer International Publishing, Berlin, Springer-Verlag, 594. https://doi.org/10.1007/978-3-319-31733-5
7. Bouazama, I., Nait Bba, A., Aabi, A., Hejja, Y., Ou Moua, S., Baidder, L., Boujamaoui, M., Mickus, K., Raji, M., Manar, A. 2023. The role of structural inheritance in the tectonic configuration of the Moroccan Meseta Coastal Block: Insights from morpho-structural and aeromagnetic data, Journal of African Earth Sciences, 205, 104978, https://doi.org/10.1016/j.jafrearsci.2023.104978
8. Chopin, F., Corsini, M., Schulmann, K., El Houicha, M., Ghienne, J.-F., Edel, J.-B. 2014. Tectonic evolution of the Rehamna metamorphic dome (Morocco) in the context of the Alleghanian-Variscan orogeny, Tectonics, 33, 1154–1177, https://doi.org/10.1002/2014TC003539
9. Cobbing, E.J., Pitfield, P.E.J., Darbyshire, D.P.F., Mallick, D.I.J. 1992. The Granites of the South-East Asian Tin Belt British Geological Survey Overseas Memoir 10, 369.
10. Cocherie, A. 2001. Datations effectuées dans le cadre du projet Maroc. Compte-rendu technique BRGM, AC/81.11.01, 7 + annexes.
11. Cudahy, T. 2011. Satellite ASTER geoscience product notes Western Australia. WA ASTER geoscience product notes, Version 1, CSIRO Earth Science and Resource Engineering Australian Resources Research Centre (ARRC), 1–23.
12. El Attari, A. 2001. Etude lithostratigraphique et tectonique des terrains paléozoïques du Môle côtier (Méseta occidentale, Maroc). Thèse Université Mohammed V, Rabat Maroc.
13. El Janati, M. 2019. Application of remotely sensed ASTER data in detecting alteration hosting Cu, Ag and Au bearing mineralized zones in Taghdout area, Central Anti-Atlas of Morocco, Journal of African Earth Sciences, 151, 95–106, https://doi.org/10.1016/j.jafrearsci.2018.12.002
14. El Mahi, B., Hoepffner, Ch., Zahraoui, M., Boushaba, A. 2000. L'évolution tectono-métamorphique de la zone hercynienne des Rehamna centraux (Maroc). Bull. Inst. Sci., Rabat, n°22 (1999–2000), 41–57.
15. El-Mimouni, M., Aarab, A., Lakhloufi, A., Hamzaoui, A., Benammi, M., Benyas, K. 2022. New targets of potential mining interest using gravimetric and satellite data: Case study of hercynian Rehamna Massif, Morocco. Iraqi Geological Journal, 55(2D), 14–26.
16. Elsaid, M., Aboelkhair, H., Dardier, A., Hermas, E., Minoru, U. 2014. Processing of multispectral ASTER data for mapping alteration minerals zones: As an aid for uranium exploration in ElmissikatEleridiya granites, Central Eastern Desert, Egypt. Open Geol J 8(1:M5), 69–83
17. Gabr, S., Ghulam, A., Kusky, T. 2010. Detecting areas of high-potential gold mineralization using ASTER data, Ore Geology Reviews, 38 59–69.
18. Hoeppfner, C. 1974. Contribution à la géologie structurale des Rehamna (Méséta marocaine méridionale); le matériel paléozoïque et son évolution hercynienne dans l'Est du Massif. Thèse 3ème cycle 92p. Université Louis-Pasteur, Strasbourg France.
19. Hoepffner, C., Houari, M.R., Bouabdelli, M. 2006. Tectonics of the North African Variscides (Morocco, western Algeria): an outline. Comptes Rendus Geoscience, 338(1–2), 25–40. https://doi.org/10.1016/j.crte.2005.11.003

20. Hoepffner C., Ouanaimi H., Michard A.. 2017. La Meseta, un terrain vagabond ou la marge fragmentée de l'Anti-Atlas ?, Géologues N 194, 19–23.
21. Jenny, P. 1974. Contribution à la géologie structurale des Rehamna (Meseta marocaine méridionale). Le matériel paléozoïque et son évolution hercynienne dans le centre du massif. Thèse 3ème cycle, Univ. Louis Pasteur, Strasbourg, 120.
22. Kalinowski, A. and Oliver, S. 2004. Aster mineral index processing manual. Remote Sensing Applications. Geoscience Australia, 36.
23. Kholaiq, M. 2017. Tectonique hercynienne et pétro-géochimie du magmatisme acido-basique du massif des Rehamna (Meseta Occidentale- Maroc), thèse 172, Université Hassan II Casablanca, Maroc.
24. Lakhloufi, A. 2002. Evolution géodynamique des bassins de Sidi Bettache et Brachwa – Maaziz et réinterprétation de l'histoire de l'orogenèse hercynienne post-viseenne au Maroc. Thèse d'état, Université Mohammed V – Agdal, Faculté des Sciences de Rabat. N d'ordre 2050.
25. Lamrani, O., Aabi, A., Boushaba, A., Seghir, M.T., Adiri, Z., Samaoui, S. 2021. Bentonite clay minerals mapping using ASTER and field mineralogical data: A case study from the eastern Rif belt, Morocco. Remote Sens. Appl. Soc. Environ. 24, 100–640.
26. Mahjoubi, E.M. 2017. Minéralisation Stannifère d'Achmmach (Massif Central Hercynien Marocain): Relations Déformation, Magmatisme et Gîtologie. Doctoral dissertation, 309, Faculty of Sciences, Moulay Ismail University, Morocco.
27. Michard, A., Soulaimani, A., Hoepffner, C., Ouanaimi, H., Baidder, L., Rjimati, E.C., Saddiqi, O. 2010. The South-Western Branch of the Variscan Belt: Evidence from Morocco, Tectonophysics 492, 1–24.
28. Ninomiya, Y. 2003. Stabilized vegetation index and several mineralogic indices defined for ASTER VNIR and SWIR data. Proceedings of IEEE International Geoscience and Remote Sensing Symposium: IGARSS'03, 3, 1552–1554.
29. Pereira, M.F., El Houicha, M., Chichorro, M., Armstrong, R., Jouhari., A., El Attari, A., Ennih, N., Silva, J.B. 2015. Evidence of a Paleoproterozoic basement in the Moroccan Variscan Belt (Rehamna Massif, Western Meseta). Precambrian Research, 268, 61–73.
30. Piqué, A., Hoepffner, C., Jenny, J., Guezou, J.C., Michard, A. 1982. Tectonique du massif hercynien des Rehamna (Maroc). Evolution de la déformation dans les zones métamorphiques hercyniennes. Notes Mém. Serv. géol. Maroc, 303, 86–129.
31. Pirajno, F. 2009. Hydrothermal processes associated with meteorite impacts. In: Hydrothermal processes and mineral systems, 1097–1130. Springer Editor.
32. Ramadan, T.M., Kontny, A. 2004. Mineralogical and Structural Characterization of alteration zones detected by orbital remote sensing at Shalatein District Area, SE Desert, Egypt. Journal of African Earth Sciences, 40, 89–99. https://doi.org/10.1016/j.jafrearsci.2004.06.003
33. Rani, N., Singh, T., Mandla, V.R. 2020. Mapping hydrothermal alteration zone through aster data in Gadag Schist Belt of Western Dharwar Craton of Karnataka, India. Environ Earth Sci 79, 526. https://doi.org/10.1007/s12665-020-09269-9
34. Razin, P., Baudin, T., Chèvremont, P., Andries, D., Youbi, N., A., Hoepffner, C., Thiéblemont, D., Chihani, E.M. 2003. Carte géologique du Maroc au 1/50 000, feuille de Jebel Kharrou. Mémoire explicatif. Notes Mém. Serv. géol. Maroc, 436 bis, 1–105.
35. Rokos, D., Argialas, D., Mavrantza, R., St.-Seymour, K., Vamvoukakis, C., Kouli, M., Lamera, S., Paraskevas, H., Karfakis, I., Denes, G. 2000. Structural analysis for gold mineralization using remote sensing and geochemical techniques in a GIS Environment: Island of Lesvos, Hellas. Natural Resources Research 9, 277–293. https://doi.org/10.1023/A:1011505326148
36. Rowan, L.C., Mars, J.C. 2003. Lithologic mapping in the Mountain Pass Area, California using advanced space borne thermal emission and reflection radiometer (ASTER) data. Remote Sens. Environ. 84, 350–366.
37. Samaoui, S., Aabi, A., Nguidi, M.A., Boushaba, A., Belkasmi, M., Baidder, L., Bba, A.N., Lamrani, O., Taadid, M., Zehni, A. 2023. Fault-controlled barite veins of the eastern Anti-Atlas (Ougnat, Morocco), a far-field effect of the Central Atlantic opening? Structural analysis and metallogenic implications. J. African Earth Sci., 104970
38. Taylor, R.G. 1979, Geology of Tin Deposits. Elsevier Scientific Publishing Company NewYork.
39. Testa, FJ., Villanueva, C., Cooke, DR., Zhang, L. 2018. Lithological and hydrothermal alteration mapping of epithermal, porphyry and tourmaline breccia districts in the Argentine Andes using ASTER Imagery. Remote Sens 10(203), 1–45. https://doi.org/10.3390/ rs10020203
40. Tuduri, J., Chauvet, A., Barbanson, L., Bourdier, J.-L., Labriki, M., Ennaciri, A., Badra, L., Dubois, M., Ennaciri-Leloix, C., Sizaret, S. 2018. The Jbel Saghro Au(–Ag, Cu) and Ag–Hg Metallogenetic Province: Product of a Long-Lived Ediacaran Tectono-Magmatic Evolution in the Moroccan Anti-Atlas. Minerals, 8, 592. https://doi.org/10.3390/min8120592
41. Zhang, T., Yi, G., Li, H., Wang, Z., Tang, J., Zhong, K., Li, Y., Wang, Q., Bie, X. 2016. Integrating data of ASTER and Landsat-8 OLI (AO) for hydrothermal alteration mineral mapping in Duolong porphyry Cu-Au deposit, Tibetan Plateau, China. Remote Sensing 8, 890. doi:10.3390/rs8110890